



A parsimonious transport model of emerging contaminants at the river network scale

Elena Diamantini¹ and Alberto Bellin¹

¹Department of Civil, Environmental and Mechanical Engineering, University of Trento, via Mesiano 77, 38123 Trento (Italy)

Correspondence: Elena Diamantini (elena.diamantini@gmail.com)

Abstract. Waters released from wastewater treatment plants (WWTPs) are a relevant source of pharmaceuticals and personal care products to the aquatic environment, since many of them are not effectively removed by the treatment system. The consumption of these products increased in the last decades and concerns have consequently risen about their possible adverse effects on the freshwater ecosystem. In this study, we present a simple, yet effective, analytical model of transport of contaminants released in surface waters by WWTPs. Transport of dissolved species is modeled by solving the Advection-Dispersion-Reaction Equation (ADRE) along the river network by using a Lagrangian approach. We applied this model to concentration data of five pharmaceuticals: diclofenac, ketoprofen, clarithromycin, sulfamethoxazole and irbesartan collected in two field campaigns, conducted in February and July 2015, in the Adige river, North-East of Italy. The model showed a good agreement with measurements and the successive application at the monthly time scale highlighted significant variations of the load due to the interplay between streamflow seasonality and variation of the anthropogenic pressure, chiefly due to the variability of touristic fluxes. Since the data required by the model are widely available, our model is suitable to large-scale applications.

1 Introduction

The presence of pharmaceuticals and personal care products (PPCPs) in the environment raises growing concerns because of their potential harmful effects on humans and freshwater ecosystems (Ebele et al., 2017). Despite these substances are ubiquitous in populated areas and detected in fresh waters with concentrations ranging from nanograms to micrograms per litre, they are not monitored on regular basis by Environmental Agencies (Heberer, 2002; Ellis, 2006; Kuster et al., 2008; Acuña et al., 2015; Rice and Westerhoff, 2017). The main entry route of PPCPs into the aquatic environment is through the water discharged by waste water treatment plants (WWTPs), whose removal efficiency varies in dependence of the type of contaminant and the treatment technology (Halling-Sørensen et al., 1998; Rivera-Utrilla et al., 2013; Petrovic et al., 2016). The ubiquitous presence of PPCPs in freshwaters is due to the rise of urban population and the continuous introduction of new products in the market, given the escalating request by human population and for livestock breeding. Persistence of PPCPs in freshwater varies from a few days to years, depending on both environmental conditions and characteristics of the compound. However, their concentration downstream the WWTPs may change significantly as an effect of dilution and environmental conditions, chiefly solar irradiation and water temperature. Situations of pseudo-persistence of supposedly rapidly degrading PPCPs due to continuous release have also been observed (Ebele et al., 2017).



Since PPCPs are designed to exert physiological effects at low dosage, possible adverse consequences on humans and biota have become an issue of increasing concern (Heron and Pickering, 2003; Schwab et al., 2005; Boxall et al., 2012): disruption of human endocrine functions, developmental defects in fish and other organism, alterations in the survival, growth, and reproduction of several species, and the promotion of antibiotic resistance are just a few examples of adverse effects requiring investigation (see e.g., Brooks et al., 2009; Corcoran et al., 2010; Hemond and Fechner, 2014; Ebele et al., 2017). As a first response to these concerns, the European Union emanated the Directive 2013/139/EU (Council of European Union, 2013) which identifies priority substances that might represent a potential risk and defines environmental quality standards.

Attempts to evaluate the propagation of PPCPs in the freshwater ecosystem have been performed by using GIS-based models, such as PhATE (Pharmaceutical Assessment and Transport Evaluation) (Anderson et al., 2004) and GREAT-ER (Geography-Referenced Regional Exposure Assessment Tool for European Rivers) (Feijtel et al., 1997). Both models take into account the decay of the species along the river in a simplified manner by considering a representative water discharge and therefore neglecting changes of dilution due to its variability in time.

The model PhATE applies mass balance at the catchment scale, i.e. by considering all the releases upstream the point of interest and estimates concentrations of active pharmaceutical products in surface waters by considering a representative water discharge (Anderson et al., 2004). It is composed of two modules: the exposure module, which estimates environmental concentrations, and the human health effect module, which deals with risk assessment (Aldekoa et al., 2015). Environmental concentrations are estimated by dividing the total WWTP load of the target compound by a representative water discharge at the point of interest. The effect of transport along the river network is therefore neglected and the water discharge is typically selected as representative of low flow conditions. In doing that, seasonal variations are neglected, thereby impairing the estimate of accumulation in the biota and the sediments. The WWTP loads are estimated as the product of the total compound consumption, given by the per capita consumption multiplied by the served population, by two reducing factors taking into account the fraction of the compound metabolized by the human organism and that removed by the WWTP.

GREAT-ER was developed for applications in large river basins at the pan-European scale (Boeije et al., 1997; Koormann et al., 2006), and it has been also applied for environmental risk assessment (Kehrein et al., 2015). The river network is divided into connected segments, each one receiving the load from upstream and from both the WWTPs and the industrial sewage systems directly connected to it. The last version of the software includes a uniformly distributed injection along the segments (Kehrein et al., 2015). The model assumes stationary (constant in time) emissions such that residence time is relevant only if decay is considered. Several types of decay are included, all lumped in a first order kinetic with the residence time estimated as the ratio between the length of the segment and a reference stationary flow velocity. Similarly to PhATE, and consistently with the hypothesis of stationary release, a single water discharge representative of low flow conditions is considered to obtain concentrations from the estimated mass flux. Stationarity of emissions and the assumption of a constant and deterministic residence time does not allow to estimate the seasonal variability of PPCPs concentrations at the selected locations. However, recognizing that uncertainty plagues parameters selection, and in an attempt to evaluate its propagation to the concentration estimates, the developers of GREAT-ER included a Monte Carlo procedure to evaluate parametric uncertainty under the assumption that the parameters are normally distributed independent random variables with given means and variances.



We propose a new modeling approach that removes the assumption of stationarity in both emissions and streamflow. In the present work transient flow conditions are modeled as a succession of stationary flows representative of seasonal variability, under the hypothesis that the residence time is smaller than the characteristic time of flow variations. This hypothesis can be removed at the price of a larger complexity of the model, which is not always justified, particularly when the objective of the analysis is the estimation of the seasonal loads, as in the present work and in most applications alike. Our model is parsimonious in terms of number of parameters, and requires streamflow and PPCPs emissions at the selected time scale, typically the daily scale. Streamflow may be obtained from recorded data or from hydrological modeling. Similarly to GREAT-ER all decay processes are lumped in a single first-order decay rate, and sorption by sediments is included through a linear equilibrium isotherm. Both the decay rate and the partition coefficient are temperature dependent through the Arrhenius law. Removing the stationary hypothesis is important in all the cases with seasonal fluctuation of water discharge and populations, the latter due to touristic fluxes, such as in the Alpine region. Indeed, the importance of transient conditions, due to variability in the consumption of PPCPs and streamflow, may be limited in large pan-European catchments but becomes more influential as the size of the catchment reduces, especially in the Alpine region where touristic fluxes causes relevant seasonal variations of the population. The effects of the above non-stationarities have been scarcely investigated (see e.g., Alder et al., 2010), since very few studies have analyzed temporal and seasonal variations (Loraine and Pettigrove, 2006; Robinson et al., 2007; Daneshvar et al., 2010; Aldekoa et al., 2015) in both predicted concentrations and in the estimation of the overall attenuation of PPCPs loads. Herein, we propose a new parsimonious, in terms of parameters, in-stream transport model which includes the concurrent effects of dilution, dispersion and decay of PPCPs in surface waters. Its strength is in the parametrization of the releases as a function of human resident population and touristic fluxes, the latter varying seasonally, both considered as a proxy of the sewage effluents. Human population and touristic fluxes data are widely available and this makes the model applicable in a variety of situations, despite the lack of systematic data on the contamination by PPCPs. Moreover, our model can be easily coupled to existing hydro-climatological models providing streamflow and water temperatures in the catchment of interest and is consistent with the general framework developed by Botter et al. (2011) under the hypothesis that the time scale of interest is larger than the residence time. For this reason we suggest our approach for estimating contaminant loads at daily time scales, or larger.

The model is presented in Sect. 2, whereas Sect. 3 describes the Adige river basin and the data used for the simulations. Section 4 discusses inference of model parameters, and finally Sect. 5 discusses the simulations performed to estimate the seasonal loads.

2 The Model

We model transport of a reactive solute along a stream of the river network by means of the following one-dimensional Advection Dispersion Reaction Equation (ADRE) (Bachmat and Bear, 1964):

$$(1 + K_d) \frac{\partial C}{\partial t} + v \frac{\partial C}{\partial x} = \alpha_L v \frac{\partial^2 C}{\partial x^2} + r \quad (1)$$



where C [ML^{-3}] is the solute concentration, x [L] is the Lagrangian coordinate measured along the stream, t [T] is time, v [LT^{-1}] is the mean velocity, α_L [L] is the local dispersivity, K_d [–] is the partition coefficient of the linear equilibrium isotherm representing sorption to the sediments, and r [$\text{ML}^{-3}\text{T}^{-1}$] is the sink/source term representing the decay due to bio-geochemical reactions occurring in the liquid phase. The solute decays according to a first-order irreversible reaction $r = -kC$, where k [T^{-1}] is the reaction rate lumping all the decay mechanisms occurring in the liquid phase. By introducing the following transformation: $C(x, t) = \tilde{C}(x, t)e^{-kt}$, Eq. (1) reduces to the classical Advection Dispersion Equation (ADE) in the transformed concentration \tilde{C} :

$$(1 + K_d) \frac{\partial \tilde{C}}{\partial t} + v \frac{\partial \tilde{C}}{\partial x} = \alpha_L v \frac{\partial^2 \tilde{C}}{\partial x^2} \quad (2)$$

We limit our attention here to flows varying over time-scales larger than the residence time of the solute within the network, thereby excluding flooding events. This approximation can be applied also to estimate solute export at the monthly time scale with the velocity v in the Eq. (1) averaged at the monthly time-scale. In addition, we assume the velocity to vary spatially according to the following power law expression proposed by Dodov and Fofoula-Georgiou (2004):

$$v_p = \Phi(A) Q_p^{\Psi(A)} \quad (3)$$

expressing the p -th quantile of the velocity v_p [m s^{-1}], as a function of the same quantile of water discharge Q_p [$\text{m}^3 \text{s}^{-1}$]. In Eq. (3), A [km^2] is the contributing area while Φ and Ψ are scaling coefficients, which do not depend on the chosen quantile. The expressions of Φ and Ψ provided by Dodov and Fofoula-Georgiou (2004), by using a dataset of 85 gauging stations in Kansas and Oklahoma, are reproduced in the Appendix A. The expression (3) is a generalization of the power law expression $v \propto Q^m$ introduced in the pioneering work of Leopold and Maddock (1953), who noticed that the exponent m varies in dependence of the contributing area. Under the commonly accepted approximation that at the network scale the contributing area increases stepwise at the nodes of the network, we therefore assume the velocity spatially uniform within the channels.

Equation (2) should be complemented with suitable initial and boundary conditions. The initial conditions are of zero concentration $C(x, 0) = 0$ and zero absorbed concentration $C^*(x, 0) = 0$ along the stream. A suitable upstream boundary condition, mimicking the typical release condition at the WWTPs and industrial sewage systems is of continuous mass flux injection $\dot{M}(t)$ [M T^{-1}] at the position x_0 . In addition, we assume that the stream is semi-indefinite with the boundary condition at $x \rightarrow \infty$ of zero flux concentration, i.e. $C_F(x, t) = \tilde{C}(x, t) - \alpha_L \partial \tilde{C}(x, t) / \partial x = 0$ for $x \rightarrow \infty$. This condition is equivalent to assuming that the downstream boundary condition does not affect mass flux.

Owing to the linearity of Eq. (2), the flux concentration C_F of the solute at a given position x along the stream assumes the following expression:

$$C_F(x, t) = \int_0^t C_{F,in}(t_0) g_M(x, t - t_0) dt_0 \quad (4)$$



where $C_{F,in} = \dot{M}(t)/Q(t)$ is the flux concentration at the injection point $x = x_0$, under the assumption that the release mass rate is \dot{M} and that mixing with stream water occurs instantaneously. In Eq. (4) the transfer function assumes the following form:

$$g_M(x, t) = g(x, t) e^{-k t} \quad (5)$$

5 with

$$g(x, t) = \frac{x - x_0}{\sqrt{4\pi\alpha_L v_R t^3}} \exp\left\{-\frac{[x - x_0 - v_R t]^2}{4\alpha_L v_R t}\right\} \quad (6)$$

being the solution of the Eq. (2) for an instantaneous mass injection such that:

$$c_F(x_0, t) = \delta(t) \quad (7)$$

10 where $c_F = \dot{M}/M = C_{F,in}/(M/Q)$ [T^{-1}] is the flux concentration for a unit ratio between the total injected mass and water discharge and $\delta(\cdot)$ [T^{-1}] is the Dirac delta function. Equation (6) is the classical solution discussed in Kreft and Zuber (1978, Eq. 11) for both injection and detection in flux and unitary ratio M/Q .

2.1 Extension to the river network

Let us consider the generic network represented in Fig. (1). The injection occurs at the position $x_{0,i}$ along the channel number i and the solute follows this path:

$$15 \quad (i, 1) \rightarrow (i, 2) \rightarrow (i, 3) \rightarrow \dots (i, j) \rightarrow \dots (i, n_i) \quad (8)$$

where (i, j) indicates the j -th channel in the ordered sequence of channels connecting the injection point to the control section CS , and n_i is the total number of elements (channels), in the sequence. The input signal at $x = x_{0,i}$ is transferred to the end of the channel $i \equiv (i, 1)$ by means of the expression (4), which can be rewritten as follows:

$$C_F(L_{(i,1)}, t) = C_{F,in}^{(i)}(t) * g_M(L_{(i,1)} - x_{0,i}, t) \quad (9)$$

20 where $C_{F,in}^{(i)}$ is the concentration flux of the solute released at the coordinate $x_{0,i}$ along the channel i of length $L_{(i,1)}$ and $*$ indicates the convolution integral of Eq. (4).

The signal arriving from the channel $(i, 1)$ is propagated to the end of the following channel (i.e. the channel $(i, 2)$) taking into account the dilution occurring at the node as an effect of the joining channel(s) (i.e. the channel l in the Fig.(1)). The same



procedure is repeated for all the channels composing the path from the source to the control section. At the j -th channel in the sequence the convolution assumes the following form:

$$C_F(L_{(i,j)}, t) = \left\{ \frac{Q_{(i,j-1)}(t)}{Q_{(i,j)}(t)} C_F(L_{(i,j-1)}, t) \right\} * g_M(L_{(i,j)}, t); \quad j = 2, \dots, n_i \quad (10)$$

Finally, owing to linearity of the transport processes, the flux concentrations $C_F(L_{(i,n_i)})$, $i = 1, \dots, N$ propagated from the N sources within the catchment are summed up to obtain the total concentration flux at the control section CS :

$$C_{F,S}(t) = \sum_{i=1}^N C_F(L_{(i,n_i)}, t) \quad (11)$$

Under the additional assumption that $\frac{Q_{(i,j-1)}(t)}{Q_{(i,j)}(t)} \simeq \frac{A_{(i,j-1)}}{A_{(i,j)}}$, where $A_{(i,j)}$ is the contributing area to the j -th channel, the sequence of convolutions assumes the following form:

$$C_F(L_{(i,n_i)}, t) = \frac{A_{(i,1)}}{A_{(i,n_i)}} g_M(L_{(i,1)} - x_{0,i}, t) * g_M(L_{(i,2)}, t) * \dots * g_M(L_{(i,n_i)}, t) * C_{F,in}^{(i)}(t) \quad (12)$$

with $A_{(i,n_i)} = A_S$, the contributing area at the control section. At the release point $x_{0,i}$ the flux concentration can be expressed as follows: $C_{F,in}^{(i)}(t) = \frac{\dot{M}_i(t)}{Q_{(i,1)}(t)}$, with \dot{M} indicating the released mass flux from the WWTP and $Q_{(i,1)} = Q_i$ is the stream water discharge at the point of release.

The released mass flux from the i -th WWTP is given by the product of the unitary released mass flux (i.e. the mass flux released per person) γ_i [$M T^{-1}$] and the population $P_i(t)$ served by the WWTP: $\dot{M}_i(t) = \gamma_i P_i(t)$.

The unitary mass flux is given by:

$$\gamma_i = \frac{\alpha_i D_i \beta_i (1 - f_i)}{\Delta T} \quad (13)$$

where α_i [-] is the assimilation factor, corresponding to the fraction of daily dose D_i [$M T^{-1}$] per person that is released by the human body, β_i [-] is the percentage of usage of the targeted active principle, $f_i < 1$ is the decay factor of the WWTP and ΔT is the transformation factor of time to make the units congruent with the time step used in the model.

The classical study by Rinaldo et al. (1991) showed that geomorphological dispersion acting at the network scale overwhelms local dispersion in shaping the hydrological response of a catchment. The same assumption, preventively verified numerically, can be introduced in our model in which dilution caused by the progressive increase of water discharge as the solute moves downstream rapidly overwhelms dilution due to local dispersion, which can be neglected by assuming $\alpha_L \rightarrow 0$. Under this condition the transfer function of the channel (i.e. Eq. (5)), with g provided by Eq. (6), reduces to:

$$g_M(x, t - t_0) = \delta[x - x_0 - v_R(t - t_0)] \exp[-k(t - t_0)] \quad (14)$$

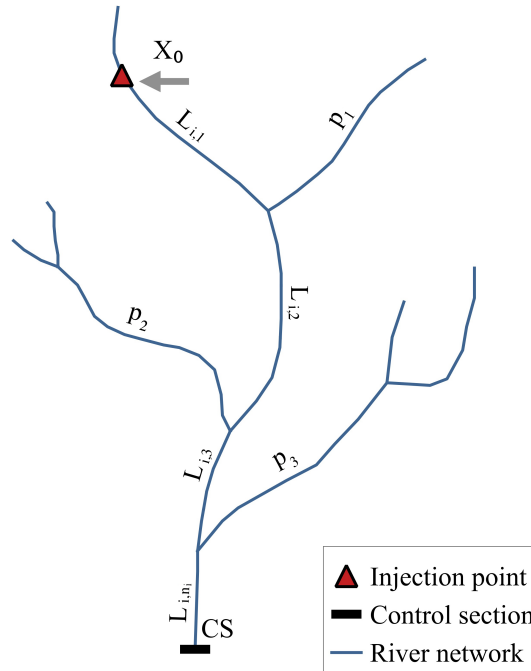


Figure 1. Sketch of the network with indicated the labeling of the streams, a release point at the Lagrangian coordinate $x_{0,i}$ along the i -th stream, and the control section (CS). The distance between the i -th release and the Control Section is defined as $\sum_{j=1}^{n_i} L_{i,j}$. Along this path, tributaries (p_1, p_2 and p_3 in figure) contribute with further water discharge, thereby causing dilution.

where $\delta [T^{-1}]$ is the Dirac Delta distribution. Neglecting α_L has the advantage of reducing by one the number of parameters that should be inferred from the data, thereby reducing the risk of over-parameterization, when, as often occurs, concentration data are scarce. The substitution of Eq. (14) into Eq. (12) leads to the following expression of the flux concentration:

$$C_F(L_{(i,n_i)}, t) = \frac{A_{(i,1)}}{A_{(i,n_i)}} C_{F,in}^{(i)} \left(t - \sum_{j=1}^{n_i} \tau_{i,j} \right) \exp \left[-k \sum_{j=1}^{n_i} \tau_{i,j} \right] \quad (15)$$

5 with the travel time $\tau_{i,j}$ of the i -th channel in the path (i.e. Eq. (8)) that assumes the following expression:

$$\tau_{i,j} = \frac{L_{(i,j)} - \delta_{1j} x_{0,i}}{v_{0,R}(A_{(i,j)})} \quad (16)$$



where the retarded velocity is given by

$$v_{0,R}(A_{(i,j)}) = \frac{1}{1 + K_d} \Phi(A_{(i,j)}) (q A_{(i,j)})^{\Psi(A_{(i,j)})} \quad (17)$$

In Eq. (17), q [$L T^{-1}$] is the specific water discharge (i.e. the water discharge per unit contributing area here considered constant through the catchment). In Eq. (16) δ_{1j} is the Kronecker delta, which is equal to 1 when $j = 1$ and zero otherwise.

5 Finally, according to the Arrhenius law, the coefficient of decay k assumes the following expression (Arrhenius, 1889):

$$k = A \exp \left[-\frac{E_A}{\mathcal{R}\theta} \right] \quad (18)$$

where A [s^{-1}] is the frequency factor, E_A [$kJ mol^{-1}$] is the activation energy, $\mathcal{R} = 8.314 * 10^{-3} kJ K^{-1} mol^{-1}$ is the gas constant and θ [K] is the water temperature. Notice that $v_{0,R}$ changes along the river network according to the contributing area.

10 3 Materials and methods

3.1 The Adige river basin

We applied our model to the Adige, a large Alpine river in the North-Eastern Italy, with the parameters inferred by means of inverse modeling applied to one of its main tributaries: the Noce river. The Adige catchment area is of 12,100 km^2 (Fig. 2) with the large majority of the basin (91%) belonging to the Trentino-Alto Adige region. The main stem has a length of 409 km from the spring to the estuary in the Adriatic sea. Along its course the river receives the contributions of Passirio, Isarco, Rienza, Noce, Avisio, Fersina and Leno (Fig. 2). Streamflow is characterized by a first maximum in spring, due to snowmelt, and a second one in autumn caused by cyclonic storms. Climate is typically Alpine and characterized by dry winters, snow and glacier-melt in spring, and humid summers and autumns (Lutz et al., 2016). The Noce river is a tributary of the Adige river. It rises from the reliefs of the Ortles-Cevedale and Adamello-Presanella groups and flows first to East, then around its middle course it turns to South-East and enters the Adige river close to the town of Mezzolombardo, North of the city of Trento (Fig. 2). Its total contributing area is of 1,367 km^2 and its total length is of 82 km (Majone et al., 2016).

3.2 Meteorological, hydrological and chemical data

Stream water of the Noce was sampled in two sampling campaigns performed respectively on February 15-17, 2015 and July 3-5, 2015 at the following sites (see Fig. 2): Tonale pass, immediately downstream the WWTP serving a large ski area (WB2B), two sites in Mezzana, immediately downstream the WWTP serving the middle val di Sole valley (WB3A and WB3B) and in two sites in the town of Mezzocorona, lower Non valley, immediately upstream and downstream the restitution of the Mezzocorona power plant (WB4B and WB5B, respectively). Details on sampling procedures, sampling locations, and

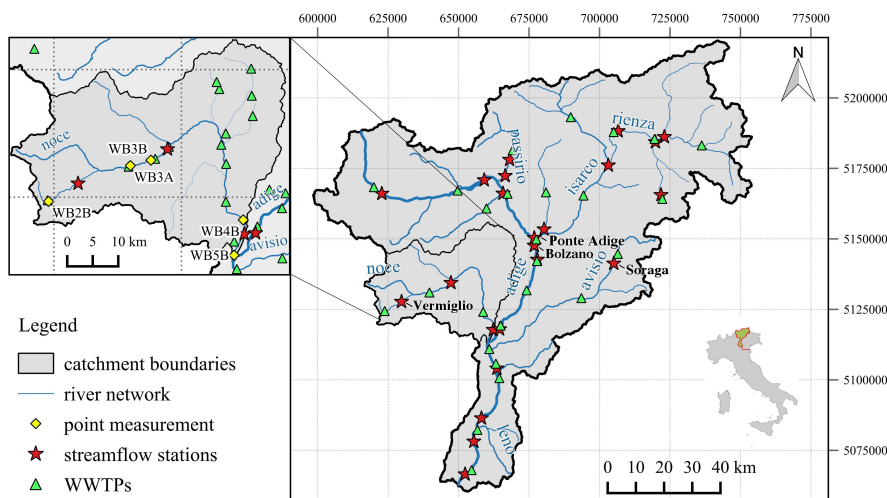


Figure 2. Map of the Adige river basin and its main tributaries with a zoom on the Noce river basin (upper left panel). Green triangles represent the main WWTPs whereas red stars indicate the gauging stations. The gauging stations used as control sections are identified with their names (i.e. Soraga, Vermiglio, Ponte Adige and Bronzolo). Only for the Noce basin, yellow diamonds shows the sampled locations during the two sampling campaigns of February and July, 2015.

analyses performed are provided in the work by Mandaric et al. (2017). These two periods were selected such as to capture extreme conditions in the catchment. Winter is the main touristic season with a large number of tourists hosted in hotels and houses in the ski area and along the Sole valley, while streamflow is at the annual minimum. On the other hand, summer is characterized by lower, yet significant, touristic presences and high streamflow due to snow melting. In the winter campaign,

5 36 out of the 80 investigated pharmaceuticals were detected in water samples with concentrations above their respective Limit Of Quantification (LOQ) whereas in the summer campaign, this number reduced to 15, and with concentrations mostly lower than in winter (Mandaric et al., 2017). Among the detected pharmaceuticals, the five with the highest concentrations in both sampling campaign were selected for simulation. They are:

- Diclofenac: non-steroidal anti-inflammatory drug with antipyretic and analgesic actions;
- 10 – Ketoprofen: non-steroidal anti-inflammatory drug, analgesic and antipyretic;
- Clarithromycin: semisynthetic macrolide antibiotic;
- Sulfamethoxazole: sulfonamide bacteriostatic antibiotic. Its broad spectrum of activity has been limited by the development of resistance;
- Irbesartan: nonpeptide angiotensin II antagonist with antihypertensive activity.



Although detected only in February, diclofenac was included because it belongs to the watch list in the directive 2013/39/EU of the European Parliament. For additional information on these compounds we refer to the PubChem Compound database (<https://pubchem.ncbi.nlm.nih.gov/compound>).

The locations of WWTPs were obtained from the local authorities responsible for urban waste water treatment in the provinces of Trento (<https://adep.provincia.tn.it/Agenzia-per-la-Depurazione-ADEP>) for Trentino Province and Bolzano (<http://www.provincia.bz.it/agenzia-ambiente/acqua/cartine-schede.asp>) for Alto Adige Province. The geometry of the river network, including the distances of the WWTPs from the control sections, were obtained from the official river network shape file, which includes deviation of the natural river courses (EU-DEM; <http://www.eea.europa.eu/data-and-maps/data/eu-dem>, <http://www.sinanet.isprambiente.it/it/sia-ispra/download-mais/reticolo-idrografico/view>). All the spatial analyses were per-

formed through QGIS (<http://www.qgis.org/it/site/>). Resident population and touristic presences were obtained from the census offices of Trento (<http://www.istat.it/it/>) and Bolzano (<https://astat.provincia.bz.it>) at annual and monthly resolution, respectively. Population was assigned to the WWTPs according to the served municipalities and resident population was assumed constant through the year.

Daily streamflow time series (Q) were obtained from the hydrological offices of the Provinces of Trento (<http://www.floods.it/public/index.php>) and Bolzano (http://www.provincia.bz.it/hydro/index_i.asp). Monthly streamflow time series at the gauging stations were then computed by aggregating daily values.

Finally, water temperatures (WT) at the streamflow gauging stations were provided by the Environmental Protection Agencies of the provinces of Trento (<http://www.appa.provincia.tn.it>) and Bolzano (<http://www.provincia.bz.it/agenzia-ambiente/>) at monthly resolution (Fig. 2). The parameters α_i , β_i and D_i of Eq. (13) are obtained from the datasets of the Collaborating Centre for Drug Statistics Methodology of the World Health Organization (<http://www.whocc.no/>) and the Italian Agency of Drug (Agenzia Italiana del Farmaco, AIFA; <https://farmaci.agenziafarmaco.gov.it/bancadatifarmaci/home>).

3.3 Inference of the model parameters

To comply with Occam's razor principle (MacKay, 2003, ch. 28), suggesting parsimony in selecting model complexity and considering the very limited amount of concentration data available, we assume that the parameters in the Eq. (13) are the same for all the WWTPs and that the abatement is zero (i.e. $f_i = 0$, $i = 1, \dots$). Hence, under these conditions $\gamma_i = \gamma$. The parameters space has been explored by Latin Hypercube sampling with the probability distribution assumed multi-log-normal with means and variances of γ and k provided in Table 1 and obtained from the pharmacological databases described in Sect. 3.2.

The inference of model's parameters was performed by using concentration measurements along the Noce river as observational variables. The unitary mass flux release γ may change seasonally as an effect of variability in drugs consumption, due to changes in touristic fluxes, while the variability of k is reproduced through the Arrhenius law (Eq. (18)). We investigated four possible models with different numbers of parameters (i.e. n_p):

- M1: a single value of γ is considered through the year and decay k is set to zero; this is a single parameter model ($n_p = 1$);



Table 1. Means ($\bar{\gamma}$) and variances (σ^2) of the log-normal distributions of the unitary mass fluxes (γ) and of the coefficients of decay (\bar{k}) for the 5 selected pharmaceuticals. The standard deviation of the associated normal distributions, with unitary means, was set equal to 3 in order to explore several order of magnitudes and, hence, all the possible physical values.

<i>Pharmaceutical</i>	$\bar{\gamma}$ [ng hab ⁻¹ d ⁻¹]	σ_{γ}^2 [ng ² hab ⁻² d ⁻²]	\bar{k} [s ⁻¹]	σ_k^2 [s ⁻²]
Diclofenac	2.09E + 06	1.37E + 14	1.87E - 05	1.23E + 03
Ketoprofen	1.19E + 06	7.82E + 13	2.00E - 05	1.31E + 03
Clarithromycin	8.98E + 06	5.90E + 14	3.25E - 03	2.13E + 05
Irbesartan	8.20E + 05	5.39E + 13	8.53E - 05	5.60E + 03
Sulfamethoxazole	4.21E + 05	2.77E + 13	4.42E - 05	2.90E + 03

- M2: two values of γ are considered, one for the winter season and the other for the summer season, $k = 0$ as for M1; therefore $n_p = 2$;
- M3: a single value of γ is considered, as in M1, while decay is assumed to vary with temperature according to the Arrhenius law (Eq. (18)). This model requires $n_p = 3$ parameters, given that the Arrhenius law depends on A and E_A ;
- 5 - M4: γ varying seasonally as in M2 and k as in M3; therefore $n_p = 4$.

Since water temperature can be safely assumed constant in each sampling campaign, with the models M3 and M4 the inversion was performed by considering two values of k , one for the winter and one for the summer seasons, as unknown instead of A and E_A , successively the inferred values were used in Eq. (18), together with the water temperature, to compute the parameters A and E_A of the Arrhenius law.

- 10 The inference was performed for each of the four selected models by searching the parameters hyperspace through the Latin Hypercube Sampling (LHS) procedure (McKay et al., 1979) with the objective to identify the set of parameters that minimizes the following weighted least-squares criterion (see e.g., Carrera and Neuman, 1986; McLaughlin and Townley, 1996; Tarantola, 2005):

$$L(a) = [z - \mathcal{F}(a)]^T C_v^{-1} [z - \mathcal{F}(a)] + [\bar{a} - a]^T C_a^{-1} [\bar{a} - a] \quad (19)$$

- 15 where a is the vector of the unknown model parameters, z is the vector containing the observational data, \mathcal{F} is the estimate of the observational data provided by the model (i.e. Eq. (15)), C_v is the diagonal matrix of the error variances, C_a is a diagonal matrix which epitomizes the effect of uncertainty associated to the prior information, and \bar{a} is the vector of the prior estimates of the model's parameters (i.e. the means reported in Table 1). In addition, the superscript T indicates the transpose of the vector. Under the commonly assumed hypothesis that the model's errors ($z - \mathcal{F}(a)$) and the residuals ($\bar{a} - a$) are both normally



distributed and independent, the minimum of the function (Eq. (19)) coincides with the Maximum of the A-Posteriori (MAP) probability distribution (McLaughlin and Townley, 1996; Rubin, 2003; Castagna and Bellin, 2009).

LHS was performed by dividing the parameters axes in N_L intervals of constant probability $1/N_L$, thereby resulting in a partition of the hypercube in $M = N_L^{n_p}$ cells. The upper limit of the cells along the axis a_j , $j = 1, \dots, n_p$ of the hypercube is
 5 obtained by inverting the cumulate of the log-normal probability density function:

$$P(a_j) = \int_0^{a_j} \frac{1}{\ln a_j \sqrt{2\pi\sigma_{y_j}^2}} \exp \left[-\frac{(\ln a_j - \bar{y}_j)^2}{2\pi\sigma_{y_j}^2} \right] da_j \quad (20)$$

at the following discrete values: $\{1/N_L, 2/N_L, \dots, (N_L - 1)/N_L, 1\}$. In Eq. (20) the first two moments assume the following expressions:

$$\bar{y}_j = \ln \left[\frac{\bar{a}_j^2}{\sqrt{\bar{a}_j^2 + C_{a,jj}}} \right], \quad \text{and} \quad \sigma_{y_j}^2 = \ln \left[1 + \frac{C_{a,jj}}{\bar{a}_j^2} \right] \quad (21)$$

10 where $C_{a,jj}$ is the j -th diagonal term of the matrix C_a . A sampling point is then generated randomly within each cell, thereby obtaining a total number of M sampling points distributed within the hypercube. The sampling point that minimizes the function $L(a)$ given by Eq. (19) is recorded together with its value and the procedure is repeated MC times, each time with a different random location within the cells. Inference is performed for each model with $M = 100$ and $MC = 10,000$. The Nash-Sutcliffe Efficiency Index (NSE; Nash and Sutcliffe, 1970) was also used as the objective function to maximize,
 15 obtaining optimal sets of parameters close to those obtained with MAP.

The choice among the four models, each one with the optimal parameter set according to MAP criterium, has been performed by using the Akaike's information criterion (AIC; Akaike, 1974), which penalizes models with more parameters (Akaike, 1987):

$$AIC = N \ln \left(\frac{[z - \mathcal{F}(a)]^T [z - \mathcal{F}(a)]}{N} \right) + 2n_p \quad (22)$$

20 where N is the number of experimental data points and n_p is the number of parameters.

The model M4 provided the highest values of AIC (217, on average for the 5 pharmaceuticals) and was therefore discarded. In this case the better fit provided by the four parameters of the model is not enough to justify a higher model complexity, according to the Akaike criterion. Also the less complex model (i.e. M1) was discarded because of the poorer fitting (AIC=206) with respect to models M2 and M3, both with a AIC approximately equal to 200. Considering the importance of the bio-
 25 geochemical decay as attenuation factor, we selected the model M3, although it is less parsimonious than model M2, which however does not include this important process. The comparison between observations and modeling results by the model M3 for the 5 selected compounds are shown in the Fig. 3 with the optimal set of parameters shown in Table 2.

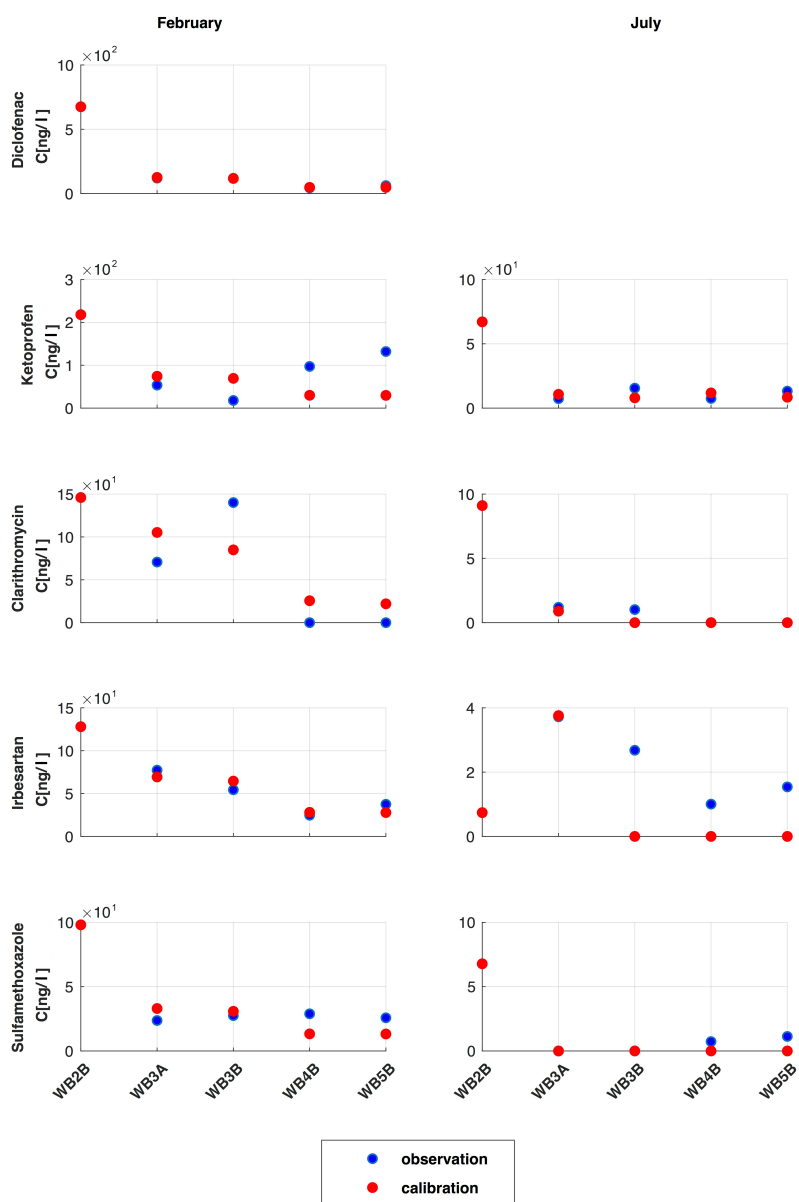


Figure 3. Concentrations of 5 selected pharmaceuticals for both winter and summer campaigns. Red bullets represent modeling results obtained with the model M3, whereas blue bullets represent measured concentrations at the 5 selected locations along the Noce river. Diclofenac was detected only during the winter campaign.



Table 2. Model M3 theoretical load coefficients (γ), coefficients of decay ($k_{february}$ and k_{july}) and L -values for the 5 pharmaceuticals.

<i>Pharmaceutical</i>	γ [ng hab ⁻¹ d ⁻¹]	$k_{february}$ [s ⁻¹]	k_{july} [s ⁻¹]	L [-]
Diclofenac	$2.03E + 06$	$1.48E - 09$	–	3.11
Ketoprofen	$1.30E + 06$	$5.00E - 09$	$3.22E - 05$	60.50
Clarithromycin	$1.95E + 06$	$1.51E - 05$	$5.49E - 03$	54.00
Irbesartan	$1.24E + 06$	$4.54E - 07$	$1.77E - 03$	71.74
Sulfamethoxazole	$5.71E + 05$	$1.39E - 08$	$3.29E - 02$	283.70

Despite the lower number of parameters, concentrations of diclofenac along the Noce river are reproduced very well by a simplified version of the model M3 with two parameters. The likelihood function is two orders of magnitude smaller than for the other compounds ($L = 3.11$, Table 2) and predicted concentrations are almost indistinguishable from the observed ones (Fig. 3). The parameters of M3 in this case are 2, instead of 3, because no diclofenac was detected in summer and therefore only the winter k value was inferred from the data. The other compounds are well reproduced by the model M3 in both seasons, except irbesartan in summer at the sampling locations WB3B, WB4B and WB5B, clarithromycin in winter and to some extent also ketoprofen in winter, particularly at the sampling locations WB4B and WB5B. The pharmaceutical with the highest L -value (i.e. the worst match with observations) is sulfamethoxazole with $L = 283.70$ (Table 2). Overall, the models succeed in representing the observed changes of PPCPs concentrations along the Noce river in both winter and summer campaigns. As expected (see Table 2), the inferred values of the decay rate k are lower in winter than in summer for all the compounds: this is due to the temperature dependence of biological processes causing degradation.

Figure 4 shows the likelihood function L given by Eq. (19) as a function of the model parameters for the model M3. In particular, L is represented in a two dimensional space as a function of γ and k , the latter being different in the two sampling campaigns (see the two columns of Fig. 4). It is worth noting that the model allowed a clear identifiability of the parameters for all the compounds, as shown by the relatively small dark blue areas corresponding to small values of L , located at large distance from the boundaries of the parameters space. As expected, the optimal k values are smaller in winter than in summer, according to water temperature being lower in winter than in summer.

4 Application at catchment scale

As an illustrative example, we applied our modeling framework to the whole Adige river with the objective of evaluating seasonal variations of PPCPs concentrations at a few relevant locations. The simulations were limited to the year 2015 for illustration purposes, but they can be extended over longer periods, including future projections, provided that hydrological and population data, both recorded or modeled, are available. The model, in particular, allows considering the interplay between

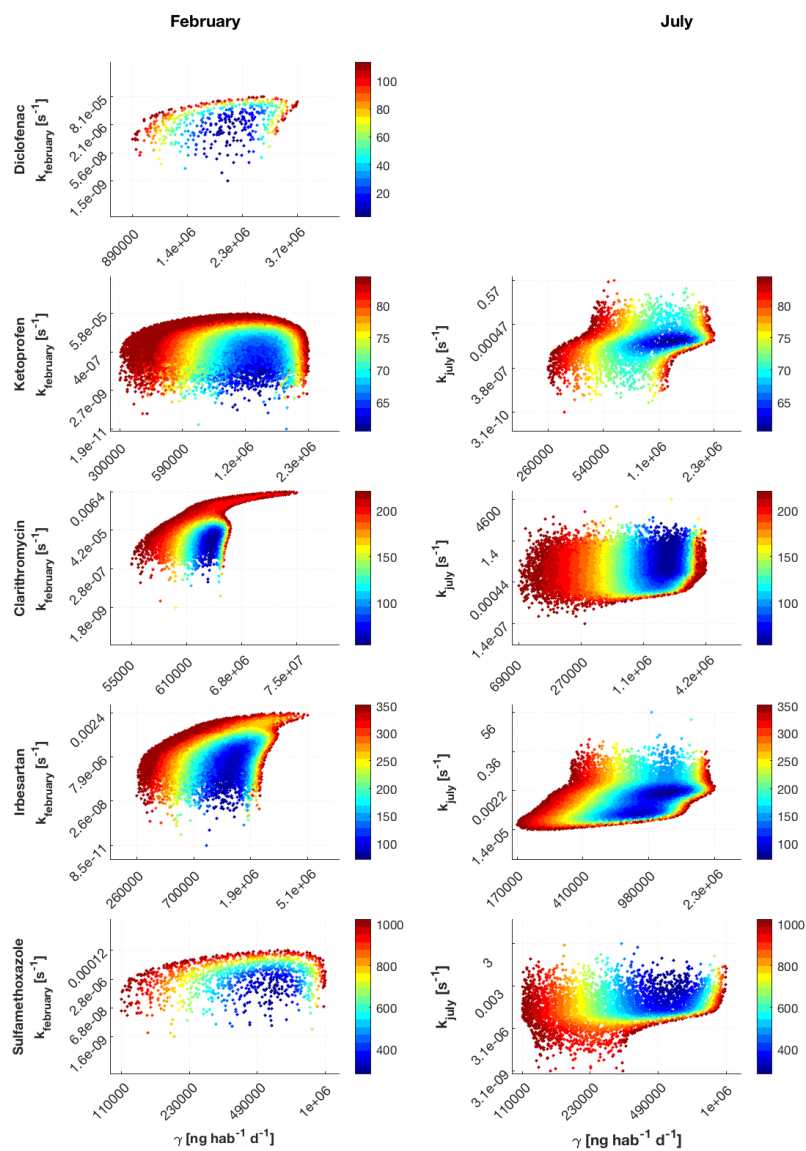


Figure 4. Objective function L , given by Eq. (19), as a function of the model's parameters for the 5 selected compounds. The left and right columns refer to winter and summer campaign, respectively. Each dot at the position sampled by the latin hypercube technique assumes the color corresponding to the scale for L shown on the right of each panel. For clarity, pairs of k and γ resulting in values of L larger than the 0.1 quantile are not shown.



Table 3. Monthly decay rates (k [s^{-1}]) of the 5 selected compounds, computed by using the Arrhenius law (Eq. (18)) with the values of A [s^{-1}] and E_A [$kJmol^{-1}$], obtained by inverting Eq. (18) with reference to the decay rate inferred from the observational data of February and July 2015 (first two rows).

	Diclofenac	Ketoprofen	Clarithromycin	Irbesartan	Sulfamethoxazole
A [s^{-1}]	$2.32E + 95$	$1.61E + 83$	$5.10E + 56$	$8.41E + 79$	$1.91E + 145$
E_A [$kJmol^{-1}$]	$5.51E + 02$	$4.84E + 02$	$3.25E + 02$	$4.56E + 02$	$8.10E + 02$
k (January) [s^{-1}]	$1.14E - 09$	$3.97E - 09$	$1.29E - 05$	$3.66E - 07$	$9.45E - 09$
k (February) [s^{-1}]	$1.48E - 09^*$	$4.99E - 09^*$	$1.51E - 05^*$	$4.54E - 07^*$	$1.39E - 08^*$
k (March) [s^{-1}]	$3.52E - 08$	$8.08E - 08$	$9.80E - 05$	$6.27E - 06$	$1.47E - 06$
k (April) [s^{-1}]	$1.74E - 07$	$3.28E - 07$	$2.52E - 04$	$2.35E - 05$	$1.53E - 05$
k (May) [s^{-1}]	$9.11E - 07$	$1.41E - 06$	$6.69E - 04$	$9.27E - 05$	$1.75E - 04$
k (June) [s^{-1}]	$2.24E - 06$	$3.10E - 06$	$1.14E - 03$	$1.95E - 04$	$6.57E - 04$
k (July) [s^{-1}]	$3.22E - 05$	$3.22E - 05^*$	$5.49E - 03^*$	$1.77E - 03^*$	$3.29E - 02^*$
k (August) [s^{-1}]	$5.49E - 06$	$6.81E - 06$	$1.93E - 03$	$4.10E - 04$	$2.45E - 03$
k (September) [s^{-1}]	$6.55E - 07$	$1.05E - 06$	$5.51E - 04$	$7.05E - 05$	$1.08E - 04$
k (October) [s^{-1}]	$8.90E - 08$	$1.82E - 07$	$1.69E - 04$	$1.35E - 05$	$5.72E - 06$
k (November) [s^{-1}]	$4.17E - 08$	$9.37E - 08$	$1.08E - 04$	$7.21E - 06$	$1.88E - 06$
k (December) [s^{-1}]	$1.14E - 09$	$3.97E - 09$	$1.29E - 05$	$3.66E - 07$	$9.45E - 09$

* inferred k values.

hydrological and population variability, the latter due to touristic fluxes evaluated at the daily scale. Simulations were performed by using the model M3 (see Sect. 3.3) with the optimal parameters shown in Table 2.

The decay rates (k), evaluated at the monthly scale, were obtained by means of the Arrhenius kinetics parameters (A and E_A), considered constant for each one of the 5 pharmaceuticals and obtained from the inversion of Eq. (18), given the two k values obtained by inversion of the observational data (see Table 3). For diclofenac the summer value of k was inherited by ketoprofen, which belongs to the same pharmacological class. Notice that k varies by orders of magnitudes (i.e. in the range $10^{-9} - 10^{-2}$ [s^{-1}]), between winter and summer, due to the seasonal fluctuations of water temperature. In winter the decay rate is rather small for all compounds, suggesting dilution as the main attenuation mechanism which, on the other hand, in winter is at its minimum due to low streamflow. In summer the decay rate is significantly higher, resulting in a concurrent effect of biological decay and dilution, which is higher than in winter due to snowmelting, for all the compounds. In terms of half-life time, July is the month with the fastest decays (half life of 6 h for diclofenac and ketoprofen, 2.1 min for clarithromycin, 6.5 min for irbesartan and 21 s for sulfamethoxazole), whereas December and January are the months with the slowest decays (half life of 19.3 y for diclofenac, 5.5 y for ketoprofen, 15 h for clarithromycin, 22 d for irbesartan and 2.3 y for sulfamethoxazole). Notice that in winter none of the 5 compounds analyzed in the present work can be considered as biologically decaying, since their half life is significantly larger than the residence time.



Only WWTPs with maximum served population higher than 10,000 persons-equivalent were selected as release points for the simulations, and communities served with systems of smaller size were aggregated to the closest selected release point. Altogether 26 WWTP release points were included into the model, obtaining a good spatial coverage (see Fig. 2). The number of persons actually served was computed at the monthly time scale based on the municipalities aggregated to each release point and the census data (including the touristic presences).

Figure 5 shows the average annual concentrations of the 5 compounds (panels from (a) to (e) in the figure) along the Adige main stem and its tributaries. The highest mean concentrations were obtained for diclofenac (panel a), particularly in the Southern and Eastern portions of the basin. The high concentrations in the upper parts of the Rienza and Avisio rivers (see Fig. 2 for the location of the Adige's tributaries) may be justified by the combined effect of low dilution and high PPCPs load due to the touristic presences, whereas the high concentrations in the lower part of the Adige main stem are due to the relatively high input loads of the city of Trento. Intermediate values were observed in the Noce upper stem and in the Adige river just upstream the city of Trento. Also ketoprofen (panel b) and irbesartan (panel d) show concentrations higher than 10^3 ng/l, both in the headwaters of the Rienza river (i.e. upper Gadera catchment), where the touristic presences are high in winter, and in the southernmost Adige main stem, downstream the confluence with the Leno river. In general, concentrations of all pharmaceuticals show a remarkable spatial variability with values ranging from 0 to $2.5E+3$ ng/l with maximum in the North-Eastern and in the Southern portions of the basin. This entails that local pharmaceutical consumption affects remarkably the detected concentrations in rivers and, in some cases, overwhelms natural dilution that acts proportionally to the water discharge.

Figure 6 shows the monthly average of flux concentrations at the following 4 selected control sections (see Fig. 2): Soraga in the upper Avisio river; Vermiglio in the Vermigliana creek (headwaters of the Noce river); Ponte Adige along the Adige river before the confluence with the Isarco river (draining the Northwestern portion of the Adige catchment) and Bolzano in the Isarco river at the confluence with the Adige river. These control sections were selected because official gauging stations with a significant drainage basin.

Diclofenac shows the highest concentrations at all gauging stations (see also the annual mean value in Fig. 5) whereas sulfamethoxazole, due to the lower input loads (see Table 2), shows the smallest concentrations. The other pharmaceuticals show temporal patterns similar to diclofenac with two peaks, one between February and March and the other in August. The dilution effect of snow melting is clearly evident in the low concentrations observed between April and June when snow-melting is at its maximum.

Vermiglio differs from the other three selected control sections: it shows a remarkable concentration peak in February, followed by a rapid attenuation in the melting season and a much less pronounced second peak in August, with respect to the other control sections. The attenuation of the second peak is justified by lower touristic fluxes with respect to winter (i.e. 30,000 persons served by the WWTP at Passo del Tonale in August 2015 against 70,000 in February of the same year) and to the streamflow contribution from summer melting of Presanella and Presena glaciers which maintains high streamflow also after the end of snowmelting season (see e.g., Chiogna et al., 2016). The simulated concentrations are higher in winter than in summer also at the control section of Bolzano. The summer peak is remarkable for diclofenac and ketoprofen, but much less

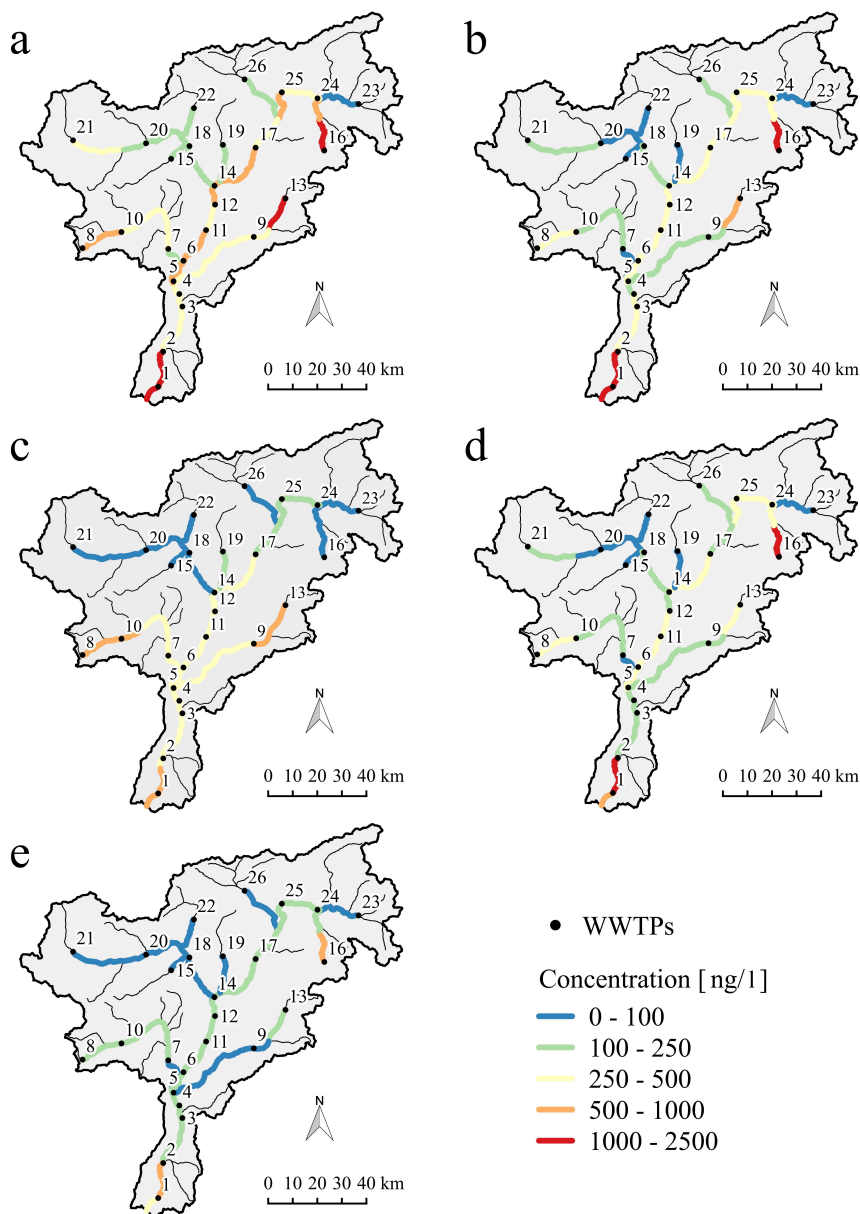


Figure 5. Annual mean concentrations of (a) diclofenac, (b) ketoprofen (c) clarithromycin (d) irbesartan (e) sulfamethoxazole in the Adige catchment for the year 2015. The position of WWTPs along the river network are marked with a black bullet and numbered progressively from the Southern control section in the main stem of the Adige river to the headwaters (see Table B1 in the Appendix B). The lowest concentrations are marked in blue, whereas the higher concentrations in red.

pronounced for the other compounds. Conversely, the highest peak at Soraga is observed in August, and this is in agreement with the higher touristic presences in summer with respect to winter (about 463 and 262 thousand persons served by the

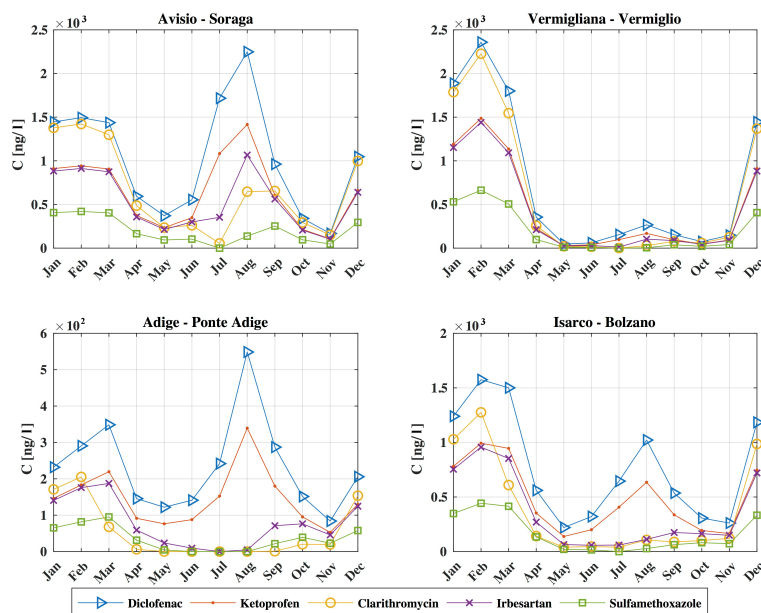


Figure 6. Monthly flux concentration of 5 PPCPs (diclofenac, ketoprofen, clarithromycin, irbesartan and sulfamethoxazole) at the control sections of Soraga in the Avisio river, Vermiglio in the Vermigliana creek, Ponte Adige in the Adige river and Bolzano in the Isarco river. Concentrations are expressed in ng/l .

upstream WWTP of Pozza di Fassa in August and February 2015, respectively), while the contribution from the Marmolada glacier is diverted outside the basin through the Fedaia reservoir (see e.g., PAT, 2012), thereby attenuating dilution. Also at Ponte Adige the summer peak was higher than in winter, showing a complex interplay between variability of streamflow and touristic presences. In addition, here the modeled concentrations are lower than in the other control sections (notice the different scales in the Fig. 6 and see also Fig. 5).

These simulations showed that concentrations of PPCPs changed through the seasons with a behavior that depends on population dynamics and hydrological characteristics of the year: a behavior that cannot be identified when a single emission and representative water discharge are adopted.

5 Discussion and Conclusions

- In the present paper we proposed a simplified, yet realistic, transport model of pharmaceuticals and personal care products in a river network. The model takes into account transient conditions of both hydrological fluxes and emissions from the waste water treatment plants and other sources, thereby overcoming the main limitations - of the existing approaches, which assume both processes as stationary. Emissions are computed by considering available data on consumption of pharmaceuticals and personal care products and population living within the catchment, including touristic fluxes, which are becoming more and



more important since touristic activities expanded tremendously in the last decades. Attenuation processes are dilution and biogeochemical decay, the former included by considering streamflow variable at the monthly scale and the latter by a first-order irreversible decay reaction.

The model was applied to the Adige river basin, North-East of Italy, by considering a selection of five pharmaceuticals, which presence was detected in two sampling campaigns conducted in February and July 2015, belonging to the groups of analgesic/anti-inflammatory, antibiotic and antihypertensive. Four different parametrizations of the model, corresponding to different hypotheses on the variability of the per-capita emission rate (i.e. γ) and the decay rate (i.e. k), have been considered and the corresponding parameters were obtained by inversion of the observational data collected in the two sampling campaigns. The best performing parametrization was identified, according to the Akaike information criterion. The selected parametrization of the model includes a constant in time γ , such that variability of the emissions follows changes in the population, which is high in the Alpine area due to important touristic fluxes in winter and summer seasons, and a decay rate k varying as a function of water temperature through the Arrhenius law. This three-parameter model has been applied at monthly time scale to the whole Adige catchment and for the year 2015. Monthly flux concentrations at four relevant gauging stations showed a significant seasonal variability as it was expected considering the large fluctuations of touristic presences and the strong seasonality of streamflow. In general, decay processes, as epitomized by the decay rate k , are less important than dilution due to both streamflow variability and the contribution from sub-catchments slightly or not impacted by pharmaceutical releases. In winter, when dilution is low the decay rate is also at its minimum because of the low water temperature, while in summer despite the decay rate is high its relevance is diminished by the overwhelming effect of dilution. Among the five selected pharmaceuticals, diclofenac and ketoprofen are those less affected by decay, while sulfamethoxazole is the compound subject to the highest decay. Overall, the proposed modeling approach shows seasonal and spatial patterns of solute concentrations in the stream water, which cannot be detected with existing approaches inherently stationary. Touristic fluxes and streamflow variability are the driving factors of these patterns, and should be carefully considered and estimated in applications. Indeed, the effects of streamflow and touristic fluctuations in the concentration patterns are intertwined, to an extent that depends on the particular compound and local conditions, and worth to be further analyzed to obtain reliable estimate of the impact on the ecosystem. Finally, our modeling framework is structured in a way that allows its use in combination with hydro-climatological models to elaborate credible future scenarios.

Code and data availability. The Matlab code of the model and the data obtained from the sampling campaigns are available upon request. All the other data needed for the reproducibility of the results are freely available and the sources are reported in Sect. 3.2.



Appendix A: Scaling coefficients of the stream velocity

Dodov and Foufoula-Georgiou (2004) proposed the following scaling laws for the coefficients Φ and Ψ of the geometry hydraulic expression of Eq. (3):

$$\Phi(A) = \exp[-(\alpha_{C_A} + \beta_{C_A} \ln(A)) + (\alpha_Q + \beta_Q \ln(A)) \Psi_{C_A}] \quad (\text{A1})$$

5 with

$$\Psi_{C_A}(A) = \left[\frac{\gamma_{C_A} + \delta_{C_A} \ln(A)}{\gamma_Q + \delta_Q \ln(A)} \right]^{1/2} \quad (\text{A2})$$

and finally the exponent Ψ is given by:

$$\Psi(A) = 1 - \Psi_{C_A}(A) \quad (\text{A3})$$

In all these expressions A [km^2] is the contributing area and the other coefficients are reproduced in the Table A1 (see also
 10 Table 3 of the paper by Dodov and Foufoula-Georgiou (2004)).

Table A1. Parameters of the scaling coefficients by Dodov and Foufoula-Georgiou (2004).

Hydraulic geometry factors	α	β	γ	δ
C_A	-3.1802	0.6124	0.8404	0.1130
Q	-5.5428	0.7992	2.6134	0.0012



Appendix B: WWTPs coordinates

Table B1. List of the WWTPs with maximum capacity of more than 10,000 person-equivalent considered in the application at catchment scale. The assigned identification numbers (ID) are sorted by latitude (from the southernmost to the northernmost plant) and the coordinates are expressed in [m] (UTM WGS 84).

<i>ID</i>	<i>Name</i>	<i>Easting</i> [m]	<i>Northing</i> [m]
1	Ala	654586	5067957
2	Rovereto	656654	5082229
3	Trento Sud	664445	5100590
4	Trento Nord	663193	5105707
5	Lavis	660857	5110902
6	Mezzocorona	664890	5119257
7	Campodenno	658702	5124097
8	Passo Tonale	623766	5124390
9	Tesero	693548	5128973
10	Mezzana	639633	5130966
11	Termeno	674101	5131753
12	Bronzolo	677758	5142131
13	Pozza di Fassa	706482	5144652
14	Bolzano	677544	5149815
15	San Pancrazio	659866	5160771
16	Sompunt	722274	5164161
17	Bassa Valle Isarco	694302	5165355
18	Merano	667329	5166009
19	Sarentino	680981	5166517
20	Media Val Venosta	649646	5167136
21	Alta Val Venosta	619907	5168345
22	Passiria	669174	5181457
23	Wasserfeld	736247	5183152
24	Tobl	719504	5185433
25	Bassa Pusteria	704999	5187904
26	Wipptal	689775	5193172



Competing interests. The authors declare that they have no conflict of interest.

Acknowledgements. This research received financial support by the European Union under the 7th Framework Programme (Grant agreement no. 603629-ENV-2013- 6.2.1-Globaqua). We thank the Environmental Protection Agencies and Hydrological and Meteorological Offices of the Autonomous Provinces of Trento and Bolzano for providing the hydrological data and the ISPAT Office of the Province of Trento
5 for providing the data on touristic fluxes. We heartfelt thanks the graduate student Deborah Bettoni for her precious collaboration in data collection and organization.



References

- Acuña, V., von Schiller, D., García-Galán, M. J., Rodríguez-Mozaz, S., Corominas, L., Petrovic, M., Poch, M., Barceló, D., and Sabater, S.: Occurrence and in-stream attenuation of wastewater-derived pharmaceuticals in Iberian rivers, *Science of the Total Environment*, 503, 133–141, 2015.
- 5 Akaike, H.: A new look at the statistical model identification, *IEEE transactions on automatic control*, 19, 716–723, 1974.
- Akaike, H.: Factor analysis and AIC, *Psychometrika*, 52, 317–332, 1987.
- Aldekoa, J., Marcé, R., and Francés, F.: Fate and Degradation of Emerging Contaminants in Rivers: Review of Existing Models, in: *Emerging Contaminants in River Ecosystems*, pp. 159–193, Springer, 2015.
- Alder, A. C., Schaffner, C., Majewsky, M., Klasmeier, J., and Fenner, K.: Fate of β -blocker human pharmaceuticals in surface water: Comparison of measured and simulated concentrations in the Glatt Valley Watershed, Switzerland, *Water research*, 44, 936–948, 2010.
- 10 Anderson, P. D., D’Aco, V. J., Shanahan, P., Chapra, S. C., Buzby, M. E., Cunningham, V. L., Duplessie, B. M., Hayes, E. P., Mastrocco, F. J., Parke, N. J., et al.: Screening analysis of human pharmaceutical compounds in US surface waters, *Environmental science & technology*, 38, 838–849, 2004.
- Arrhenius, S.: Über die Reaktionsgeschwindigkeit bei der Inversion von Rohrzucker durch Säuren, *Zeitschrift für physikalische Chemie*, 4, 226–248, 1889.
- 15 Bachmat, Y. and Bear, J.: The general equations of hydrodynamic dispersion in homogeneous, isotropic, porous mediums, *Journal of Geophysical Research*, 69, 2561–2567, <https://doi.org/10.1029/JZ069i012p02561>, <http://dx.doi.org/10.1029/JZ069i012p02561>, 1964.
- Boeije, G., Vanrolleghem, P., and Matthies, M.: A geo-referenced aquatic exposure prediction methodology for ‘down-the-drain’ chemicals, *Water science and technology*, 36, 251–258, 1997.
- 20 Botter, G., Bertuzzo, E., and Rinaldo, A.: Catchment residence and travel time distributions: The master equation, *Geophysical Research Letters*, 38, <https://doi.org/10.1029/2011GL047666>, <https://agupubs.onlinelibrary.wiley.com/doi/abs/10.1029/2011GL047666>, 2011.
- Boxall, A. B., Rudd, M. A., Brooks, B. W., Caldwell, D. J., Choi, K., Hickmann, S., Innes, E., Ostapyk, K., Staveley, J. P., Verslycke, T., et al.: Pharmaceuticals and personal care products in the environment: what are the big questions?, *Environmental health perspectives*, 120, 1221, 2012.
- 25 Brooks, B. W., Huggett, D. B., and Boxall, A.: Pharmaceuticals and personal care products: research needs for the next decade, *Environmental Toxicology and Chemistry*, 28, 2469–2472, 2009.
- Carrera, J. and Neuman, S. P.: Estimation of Aquifer Parameters Under Transient and Steady State Conditions: 1. Maximum Likelihood Method Incorporating Prior Information, *Water Resources Research*, 22, 199–210, <https://doi.org/10.1029/WR022i002p00199>, <http://dx.doi.org/10.1029/WR022i002p00199>, 1986.
- 30 Castagna, M. and Bellin, A.: A Bayesian approach for inversion of hydraulic tomographic data, *Water Resources Research*, 45, 2009.
- Chiogna, G., Majone, B., Paoli, K. C., Diamantini, E., Stella, E., Mallucci, S., Lencioni, V., Zandonai, F., and Bellin, A.: A review of hydrological and chemical stressors in the Adige catchment and its ecological status, *Science of The Total Environment*, 540, 429–443, 2016.
- Corcoran, J., Winter, M. J., and Tyler, C. R.: Pharmaceuticals in the aquatic environment: a critical review of the evidence for health effects in fish, *Critical reviews in toxicology*, 40, 287–304, 2010.
- 35 Council of European Union: Council regulation (EU) no 139/2013, <http://eur-lex.europa.eu/legal-content/EN/TXT/?uri=CELEX>



- Daneshvar, A., Svanfelt, J., Kronberg, L., Prévost, M., and Weyhenmeyer, G. A.: Seasonal variations in the occurrence and fate of basic and neutral pharmaceuticals in a Swedish river–lake system, *Chemosphere*, 80, 301–309, 2010.
- Dodov, B. and Foufoula-Georgiou, E.: Generalized hydraulic geometry: Derivation based on a multiscaling formalism, *Water Resources Research*, 40, n/a–n/a, <https://doi.org/10.1029/2003WR002082>, <http://dx.doi.org/10.1029/2003WR002082>, w06302, 2004.
- 5 Ebele, A. J., Abdallah, M. A.-E., and Harrad, S.: Pharmaceuticals and personal care products (PPCPs) in the freshwater aquatic environment, *Emerging Contaminants*, 3, 1 – 16, <https://doi.org/https://doi.org/10.1016/j.emcon.2016.12.004>, <http://www.sciencedirect.com/science/article/pii/S2405665016300488>, 2017.
- Ellis, J. B.: Pharmaceutical and personal care products (PPCPs) in urban receiving waters, *Environmental pollution*, 144, 184–189, 2006.
- Feijtel, T., Boeije, G., Matthies, M., Young, A., Morris, G., Gandolfi, C., Hansen, B., Fox, K., Holt, M., Koch, V., et al.: Development of a
10 geography-referenced regional exposure assessment tool for European rivers-GREAT-ER contribution to GREAT-ER# 1, *Chemosphere*, 34, 2351–2373, 1997.
- Halling-Sørensen, B., Nielsen, S. N., Lanzky, P., Ingerslev, F., Lützhøft, H. H., and Jørgensen, S.: Occurrence, fate and effects of pharmaceutical substances in the environment-A review, *Chemosphere*, 36, 357–393, 1998.
- Heberer, T.: Occurrence, fate, and removal of pharmaceutical residues in the aquatic environment: a review of recent research data, *Toxicology Letters*, 131, 5 – 17, [https://doi.org/https://doi.org/10.1016/S0378-4274\(02\)00041-3](https://doi.org/https://doi.org/10.1016/S0378-4274(02)00041-3), <http://www.sciencedirect.com/science/article/pii/S0378427402000413>, 2002.
- 15 Hemond, H. F. and Fechner, E. J.: *Chemical fate and transport in the environment*, Elsevier, 2014.
- Heron, R. and Pickering, F.: Health effects of exposure to active pharmaceutical ingredients (APIs), *Occupational Medicine*, 53, 357–362, 2003.
- 20 Kehrein, N., Berlekamp, J., and Klasmeier, J.: Modeling the fate of down-the-drain chemicals in whole watersheds: New version of the GREAT-ER software, *Environmental Modelling & Software*, 64, 1 – 8, <https://doi.org/https://doi.org/10.1016/j.envsoft.2014.10.018>, <http://www.sciencedirect.com/science/article/pii/S1364815214003089>, 2015.
- Koormann, F., Rominger, J., Schowanek, D., Wagner, J.-O., Schröder, R., Wind, T., Silvani, M., and Whelan, M.: Modeling the fate of down-the-drain chemicals in rivers: an improved software for GREAT-ER, *Environmental Modelling & Software*, 21, 925–936, 2006.
- 25 Kreft, A. and Zuber, A.: On the physical meaning of the dispersion equation and its solutions for different initial and boundary conditions, *Chemical Engineering Science*, 33, 1471–1480, 1978.
- Kuster, M., de Alda, M. J. L., Hernando, M. D., Petrovic, M., Martín-Alonso, J., and Barceló, D.: Analysis and occurrence of pharmaceuticals, estrogens, progestogens and polar pesticides in sewage treatment plant effluents, river water and drinking water in the Llobregat river basin (Barcelona, Spain), *Journal of hydrology*, 358, 112–123, 2008.
- 30 Leopold, L. B. and Maddock, T.: *The hydraulic geometry of stream channels and some physiographic implications*, vol. 252, US Government Printing Office, 1953.
- Loraine, G. A. and Pettigrove, M. E.: Seasonal variations in concentrations of pharmaceuticals and personal care products in drinking water and reclaimed wastewater in southern California, *Environmental Science & Technology*, 40, 687–695, 2006.
- Lutz, S. R., Mallucci, S., Diamantini, E., Majone, B., Bellin, A., and Merz, R.: Hydroclimatic and water quality trends across three Mediterranean river basins, *Science of the Total Environment*, 571, 1392–1406, 2016.
- 35 MacKay, D. J. C.: *Chemical fate and transport in the environment*, Cambridge University Press, Cambridge, UK, 2003.
- Majone, B., Villa, F., Deidda, R., and Bellin, A.: Impact of climate change and water use policies on hydropower potential in the south-eastern Alpine region, *Science of the Total Environment*, 543, 965–980, 2016.



- Mandarić, L., Diamantini, E., Stella, E., Cano-Paoli, K., Valle-Sistac, J., Molins-Delgado, D., Bellin, A., Chiogna, G., Majone, B., Diaz-Cruz, M. S., et al.: Contamination sources and distribution patterns of pharmaceuticals and personal care products in Alpine rivers strongly affected by tourism, *Science of The Total Environment*, 590, 484–494, 2017.
- McKay, M. D., Beckman, R. J., and Conover, W. J.: Comparison of three methods for selecting values of input variables in the analysis of
5 output from a computer code, *Technometrics*, 21, 239–245, 1979.
- McLaughlin, D. and Townley, L. R.: A Reassessment of the Groundwater Inverse Problem, *Water Resources Research*, 32, 1131–1161, <https://doi.org/10.1029/96WR00160>, <http://dx.doi.org/10.1029/96WR00160>, 1996.
- Nash, J. E. and Sutcliffe, J. V.: River flow forecasting through conceptual models part I—A discussion of principles, *Journal of hydrology*, 10, 282–290, 1970.
- 10 PAT, P. A. d. T.: Bilanci idrici - Relazione Tecnica - Il bacino dell'AVISIO, Trento. URL: <http://pguap.provincia.tn.it/>, 2012.
- Petrovic, M., Sabater, S., Elozegi, A., and Barceló, D.: Emerging Contaminants in River Ecosystems, *The Handbook of Environmental Chemistry*, 46, 2016.
- Rice, J. and Westerhoff, P.: High levels of endocrine pollutants in US streams during low flow due to insufficient wastewater dilution, *Nature Geoscience*, 10, 587–591, 2017.
- 15 Rinaldo, A., Marani, A., and Rigon, R.: Geomorphological dispersion, *Water Resources Research*, 27, 513–525, <https://doi.org/10.1029/90WR02501>, <http://dx.doi.org/10.1029/90WR02501>, 1991.
- Rivera-Utrilla, J., Sánchez-Polo, M., Ferro-García, M. Á., Prados-Joya, G., and Ocampo-Pérez, R.: Pharmaceuticals as emerging contaminants and their removal from water. A review, *Chemosphere*, 93, 1268–1287, 2013.
- Robinson, P. F., Liu, Q.-T., Riddle, A. M., and Murray-Smith, R.: Modeling the impact of direct phototransformation on predicted environ-
20 mental concentrations (PECs) of propranolol hydrochloride in UK and US rivers, *Chemosphere*, 66, 757–766, 2007.
- Rubin, Y.: *Applied stochastic hydrology*, Oxford University Press, Oxford, 2003.
- Schwab, B. W., Hayes, E. P., Fiori, J. M., Mastrocco, F. J., Roden, N. M., Cragin, D., Meyerhoff, R. D., Vincent, J., and Anderson, P. D.: Human pharmaceuticals in US surface waters: a human health risk assessment, *Regulatory Toxicology and Pharmacology*, 42, 296–312, 2005.
- 25 Tarantola, A.: *Inverse Problem Theory and Methods for Model Parameter Estimation*, SIAM, Philadelphia, 2005.